SOLAR CYCLE VARIATIONS OF THE SOLAR WIND

N. U. Crooker
Department of Atmospheric Sciences
University of California, Los Angeles, CA 90024

ABSTRACT

Throughout the course of the past one and a half solar cycles, solar wind parameters measured near the ecliptic plane at 1 AU varied in the following way: Speed and proton temperature have maxima during the declining phase and minima at solar minimum and are approximately anti-correlated with number density and electron temperature, while magnetic field magnitude and relative abundance of helium roughly follow the sunspot cycle. These variations are described in terms of the solar cycle variations of coronal holes, streamers, and transients. The solar wind signatures of the three features are discussed in turn, with special emphasis on the signature of transients, which is still in the process of being defined. It is proposed that magnetic clouds be identified with helium abundance enhancements and that they form the head of a transient surrounded by streamer-like plasma, with an optional shock front. It is stressed that relative values of a parameter through a solar cycle should be compared beginning with the declining phase, especially in the case of magnetic field magnitude.

INTRODUCTION

Not long ago very little was understood about solar cycle variations of the solar wind. The observed variations near Earth's orbit had been disappointingly small through the maximum of sunspot cycle 20. It was only when first papers appeared on the occurrence of the large, stable high-speed streams during the declining phase of cycle 20 (Krieger et al., 1973; Bame et al., 1976; Gosling et al., 1976) that it became clear that the solar wind could change appreciably over the long term. Since then our understanding of changing coronal and solar wind structure through the solar cycle has grown rapidly (Hundhausen, 1979). As suggested by Borrini et al. (1983) for helium abundance, the large scale patterns of change in other solar wind parameters over the solar cycle may be relatively well-understood as reflections of the solar cycle variations of three major coronal features: the large stable equatorial excursions of polar coronal holes which peak in the declining phase (e.g., Hundhausen, 1977), the equatorial streamer belt at solar minimum (e.g., Gosling et al., 1981), and coronal transients at solar maximum (e.g., Hildner et al., 1976). The solar wind signature of each feature and how these signatures fit into the pattern of solar cycle variations in the ecliptic plane at 1 AU are discussed below.

CORONAL HOLE SIGNATURES

Of the three signatures under consideration, the high speed stream signature of flow from coronal holes has been studied the most extensively and is the most well-established. For example, an entire monograph has been written on the subject of coronal holes and transients (Zirker, 1977).

The occurrence of high-speed streams during the declining phase of solar cycle 20 is illustrated in the 27-day Bartels format in Figure 1, which is a black-and-white reproduction of a colored figure from Feldman et al. (1979). Although the colored version conveys information more readily, and the interested reader

is urged to refer to it, the major features discussed below are apparent in the black-and-white version. Each shaded square represents a daily average of a solar wind plasma parameter. The averages range from their lowest values in black (unfortunately indistinguishable here from missing values) through shades of gray to their highest values in white. In each block, representing a different parameter, the daily squares are arranged in 27-day columns. Time increases from bottom to top in each column and from left to right across the figure.

Figure 1. Daily averages of solar wind proton bulk speed, density, and temperature and electron temperature arranged in sequential strips of 27-day Carrington rotations, with values increasing from dark to light shades, after Feldman et al. (1979). (See their colored version and code table for quantitative information.)

In the top block the two bright patches extending from the end of 1973 through 1975 are formed by two velocity peaks which recurred with every 27-day rotation of the sun. These two streams emanated from two large, stable, offset, polar coronal holes, one in each hemisphere (e.g., Hundhausen, 1977). The remaining blocks show how other plasma parameters vary in the stream structure. In the high-speed region, the proton temperature is high, while the density and electron temperature are low. In general the solar wind speed and proton temperature vary in the same way and are anticorrelated with the density and electron temperature. This is most obvious in the high-speed stream structure, but it is also the trend in the remaining portions of the diagram. The second and fourth blocks have the overall appearance of negatives of the first and third blocks.

Figure 2, also adapted from Feldman et al. (1979), is a plot of half-year averages of the parameters in Figure 1, with sunspot number plotted at the top for reference. It is clear that the characteristics of the high-speed flow from the stable coronal holes dominate the solar cycle variations of these parameters during the latter part of the declining phase of the sunspot cycle; the speed and proton temperature reach their highest values, and the density and electron temperature are depressed.

STREAMER SIGNATURES

The tendency for speed and proton temperature to be anticorrelated with density and electron temperature, as noted in Figure 1, also is apparent in Figure 2. Soon after sunspot minimum, in contrast to the declining phase, speed and proton temperature are low, and density and electron temperature are high. These are characteristics of the flow between the high-speed streams in Figure 1, and they come to dominate the solar cycle variations of the parameters as the stream signatures decline.

Recently the low-speed flow between streams has been identified as the signature of coronal streamers (Borrini et al., 1981; Feldman et al., 1981; Gosling et al., 1981). Throughout most of the solar cycle the heliospheric current sheet encircles the sun and separates magnetic fields of opposite polarity, which are carried outward by solar wind flow from polar coronal holes (e.g., Schulz, 1973; Svalgaard et al., 1975; Hundhausen, 1977; Smith et al., 1978; Hundhausen et al., 1981). The current sheet is embedded in a coronal streamer belt. Its projection onto a sphere at 1 AU is shown schematically in Figure 3, from Gosling
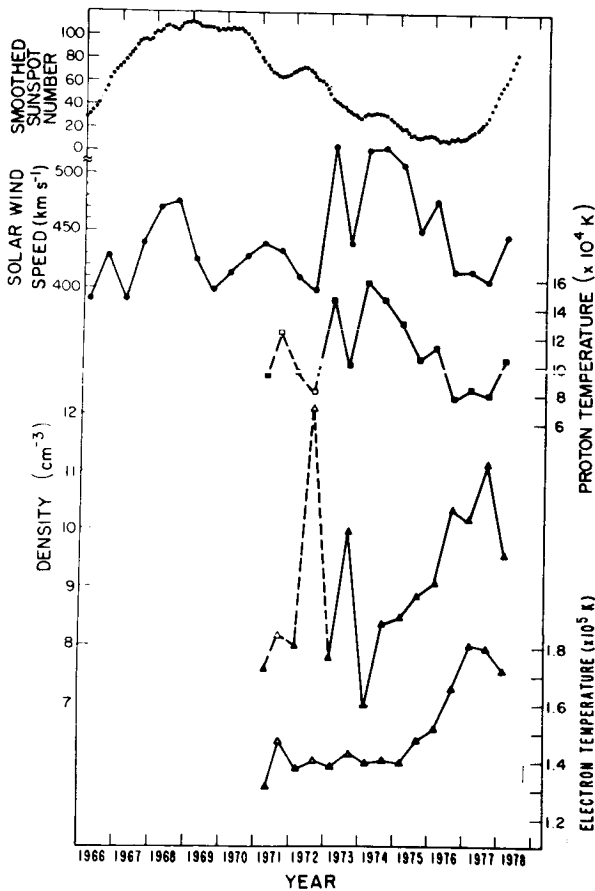

Fig. 2. Variations over the past solar cycle of monthly averages of the smoothed sunspot number and 6-monthly averages of proton bulk speed, temperature, and density and electron temperature, after Feldman et al. (1979).
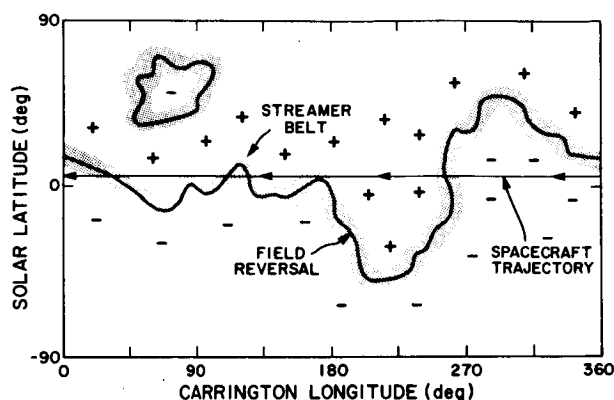
Figure 3. Schematic diagram of the intersection of the equatorial streamer belt and embedded heliospheric current sheet with the 1 AU sphere, from Gosling et al. (1981).

et al. (1981). The line labeled spacecraft trajectory shows the position of a near-Earth spacecraft as the sun completes one full rotation. During the declining phase of the solar cycle, the streamer belt makes large excursions from the solar equatorial plane, as on the right side of the figure, and an Earth-orbiting spacecraft would spend little time within it. On the other hand, during solar minimum, the streamer belt is confined to lower latitudes, as on the left side of the figure, and an Earth-orbiting spacecraft would skim and intersect it often.

The plasma signature of the streamer material surrounding the current sheet is shown in Figure 4, from Gosling et al. (1981), adapted from Borrini et al. (1981). The plots are the result of a superposed epoch analysis centered on the times of current sheet crossings. In order to obtain a clear signature, only crossings well-separated from stream interaction regions were used. The figure shows that the streamer signature has low proton temperature and flow speed and high density, which are the same extrema reached just after solar minimum in the solar cycle variations of these parameters in Figure 2. Figure 4 also shows that the relative abundance of helium (A(He)) is low in the streamer. The solar cycle variation of A(He) will be discussed in the next sections.
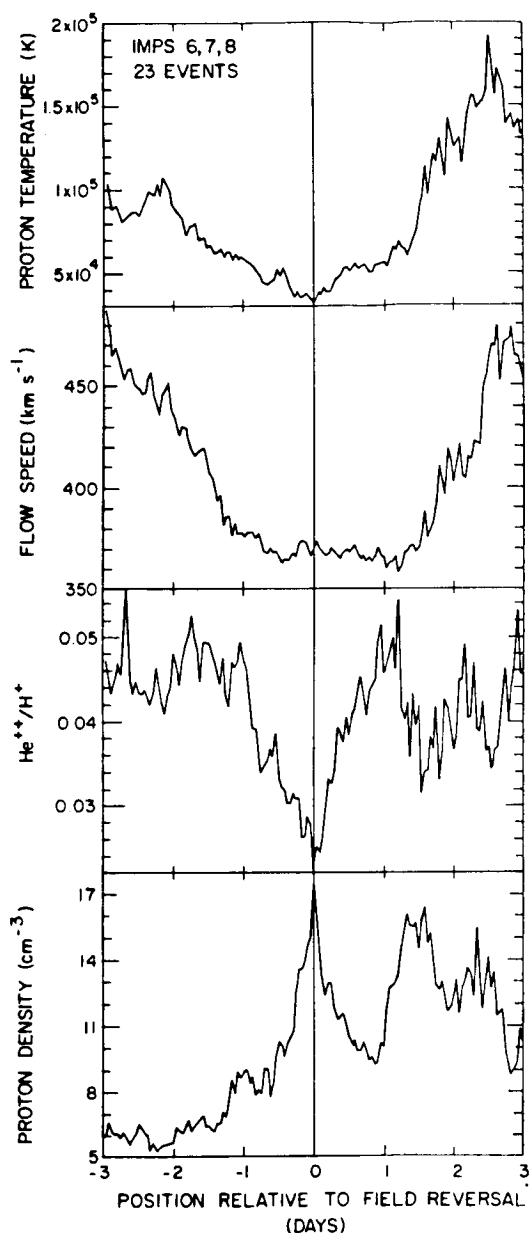

Figure 4. Superposed epoch plots of solar wind proton temperature, flow speed, helium abundance, and proton density centered on 23 well-defined current sheet crossings more than one day removed from speed rises associated with high speed streams, from Gosling et al. (1981), after Borrini et al. (1981).

In contrast to the relatively well-defined solar wind signatures of coronal holes and streamers, the signature of coronal transients is still in the process of being defined. A simple synthesis of proposed transient features is given here.

Transients have been associated with shock waves (e.g., Borrini et al., 1982a), helium abundance enhancements (e.g., Borrini et al., 1982b), non-compressive density enhancements (Gosling et al., 1977), and magnetic bottles, bubbles, and clouds (e.g., Klein and Burlaga, 1982). Figure 5 shows two examples of these transient associated signatures. Both are the results of superposed epoch analyses. The shaded regions in Figure 5a give the signature of a magnetic cloud (Klein and Burlaga, 1982). A cloud is characterized by an increase in magnetic field strength and a large excursion in the north-south field angle θ, consistent with the configuration of a magnetic loop. The plasma speed in the cloud is relatively steady, there is a small density peak at the leading edge, and the temperature is somewhat depressed. Figure 5b gives the plasma and field strength signatures accompanying an enhancement in A(He) (Borrini et al., 1982b). Similar to the characteristics of a magnetic cloud, the enhancement lasts for about one day, is preceded by a density peak, and is a region of high magnetic field strength and depressed temperature. The high degree of similarity in the signatures suggests that helium enhancements may be identified with magnetic clouds.
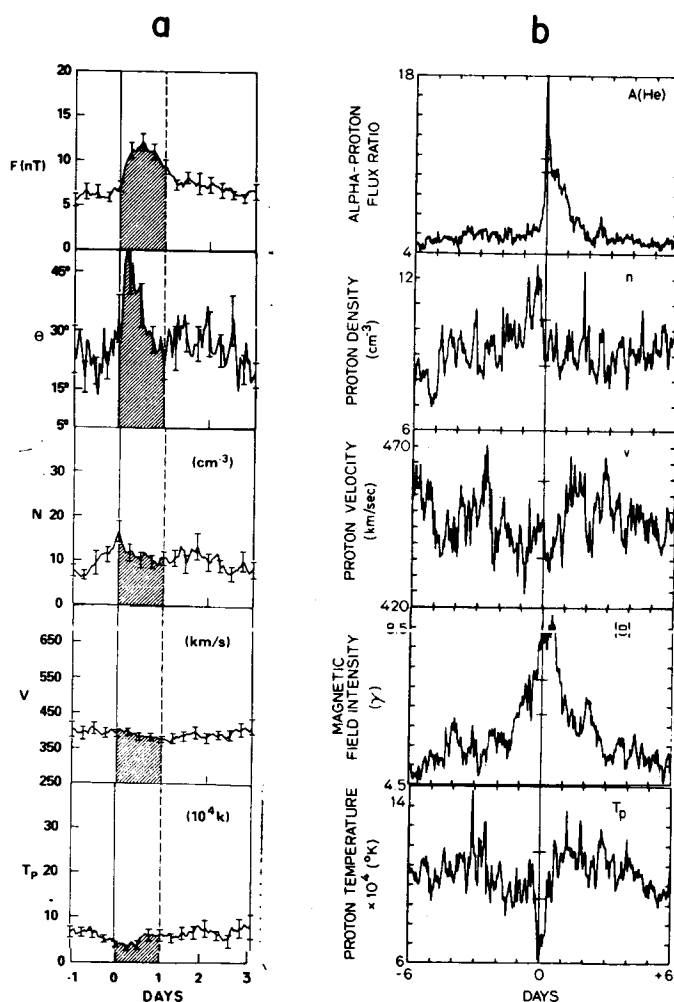
Figure 5. Superposed epoch plots of selected solar wind parameters for a.) magnetic clouds, after Klein and Burlaga (1982) and b.) helium abundance enhancements, after Borrini et al. (1982b). The parameters are magnetic field magnitude F and $|B|$, magnitude of the magnetic field angle θ of elevation out of the ecliptic plane, proton density N and n, bulk speed V and v, temperature T_p, and helium abundance A(He).

A schematic drawing of a coronal transient is shown in Figure 6. It is patterned after Hundhausen's (1972) diagram of the flare-associated, shock-wave disturbance which traditionally has been considered as the source of nonrecurrent geomagnetic activity at sunspot maximum. It incorporates the identification of a helium enhancement with a magnetic cloud, as discussed above. The cloud has a shape similar to the magnetic bubbles near 1 AU modeled by Newkirk

307

Coronal Transient

Possible Shock Front

Ecliptic Plane

Helium–rich
Magnetic Cloud

Sun

Streamer-like
Plasma

0   0.5   I AU

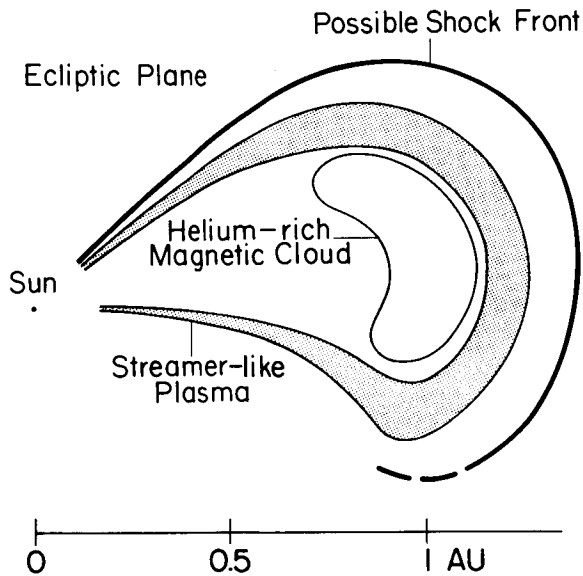Fig. 6. Schematic diagram of a cross-section of a coronal transient in the ecliptic plane. The helium abundance enhancement is identified with a magnetic cloud, and the formation of a shock front depends upon the speed of the transient relative to the ambient solar wind.

et al. (1981). Its dimension in the radial direction is about 0.25 AU, consistent with observations (Klein and Burlaga, 1982).

The streamer-like plasma surrounding the transient is drawn as an extended version of the transient configuration observed in the white-light coronographs from Skylab (e.g., Gosling et al., 1974). It may give the signature of a noncompressive density enhancement (NCDE) with elevated helium content because of its closed magnetic bottle configuration, in contrast with streamers, which have low helium content and occur on open field lines. Gosling et al. (1981) noted that streamer signatures are identical to NCDE signatures except that NCDEs occur both with high and low A(He), whereas streamers always have low A(He). They suggested that NCDEs with high A(He) may be associated with transients, consistent with the interpretation presented here. The density peak which occurs at the leading edge of the magnetic cloud and the A(He) enhancement signature in Figure 5 also is consistent with this interpretation. Outside the streamer-like plasma the magnetic field lines are open. Thus, if a shock is present, the "sheath" region between the shock and the bubble would contain first a layer with normal A(He) followed by a layer with increased A(He). The highest A(He) would then occur within the cloud. Of course, caution must be used in interpreting literally such a simple schematic diagram. Observations of transient signatures in the solar wind show a wide range of variability (e.g., Zwickl et al., in these Proceedings).

The shock front in Figure 6 is optional, depending upon the relative speed of the transient material. This option is consistent with the finding that only about half of the observed helium enhancements occur with shocks (Borrini et al., 1982b). It also has been found that only about half of the observed shocks are followed by helium enhancements (Borrini et al., 1982a). Assuming that all shocks are signatures of coronal transients and that all transients have helium enhancements, these authors suggest that the observations of shocks without helium enhancements were made by spacecraft intersecting the flanks of the shock wave and missing the central gases in the transient. If the highest concentrations of helium are confined by the closed magnetic field configuration of a magnetic cloud, as pictured in Figure 6, then this suggestion seems highly plausible.

The identification of the helium enhancement with a magnetic cloud helps to explain the result of Borrini et al. (1982a) that shocks observed with helium enhancements produce much more pronounced geomagnetic storms than do shocks without

helium enhancements. The magnetic field just inside a cloud passing over a space-craft has either a large northward or southward component which then rotates by nearly 180° (Klein and Burlaga, 1982; Smith, 1983). In either case a period of strong southward field occurs, and such periods are correlated with geomagnetic storms (e.g., Russell et al., 1974).

If it is assumed that magnetic clouds form the heart of transients and produce geomagnetic storms and that shocks produce sudden commencements, then varying the characteristics of coronal transient passage can account for the observed combinations in which these ground-based signatures occur: Central passage of transients with and without shocks will produce storms with sudden and gradual commencements, respectively, and peripheral passage of transients with shocks will produce sudden commencements or impulses without subsequent storms.

The solar cycle variation of coronal transients is inferred to be in phase with the sunspot cycle, following the solar cycle variation of geomagnetic sudden commencements, although direct measurements of the transient occurrence cycle is still incomplete (e.g., Hundhausen, in these Proceedings). Clearly the solar wind signature of coronal transients is the most complicated of the three which have been discussed, and it may be too soon to draw conclusions about their effect on solar cycle variations. Nevertheless, the somewhat irregular and intermediate averages of solar wind speed, and, by inference, density and temperatures, which occurred during sunspot maximum (see Figure 2) are consistent with the sporadic flow of intermediate-speed, shock-associated transients in a background of lower speed flow.
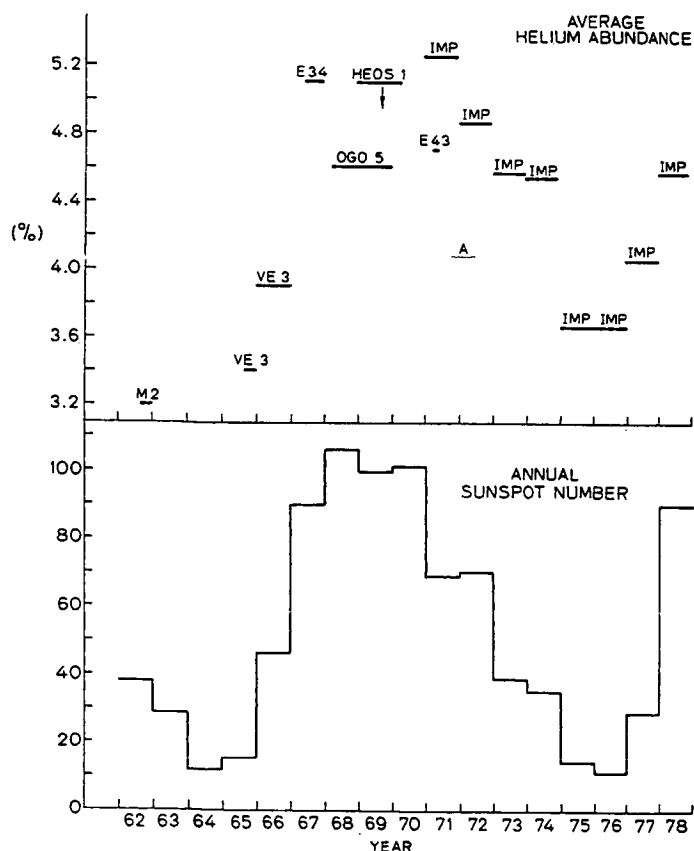
HELIUM ABUNDANCE AND MAGNETIC FIELD MAGNITUDE

Unlike the solar cycles of the plasma parameters in Figure 2, the solar cycles of A(He) and magnetic field magnitude roughly follow the sunspot cycle. Figure 7 from Borrini et al. (1983) shows the solar cycle variation of A(He), along with the sunspot cycle for reference. The figure is an extension of a previous analysis by Ogilvie and Hirshberg (1974). At sunspot maximum the averages are high, as observed in coronal transient signatures; at minimum they are low, as in streamer signatures.

This consistency does not imply that transient and streamer signatures fill most of interplanetary space in the ecliptic plane during these respective phases, as high speed stream signatures do during the declining phase. Rather the

Figure 7. Variation of relative helium abundance in the solar wind over the past solar cycle, compared with sunspot cycle, from Borrini et al. (1983).

ANNUAL AVERAGES OF IMF MAGNITUDE LOGARITHMS

Figure 8.   Variation of interplanetary magnetic field (IMF) magnitude logarithms over the past solar cycle, from King (1981). The number of hours in each yearly average are given at the bottom of the plot. Vertical bars show standard errors, and horizontal bars show portion of year for which data are available.

relatively low occurrence rate of streamers and streams and increased occurrence rate of transients during maximum result in relatively high values of A(He) at that time. The reversed relative occurrence rates of streamers and transients result in low values of A(He) at solar minimum.

During the declining phase of the past solar cycle, A(He) in the high speed streams was observed to be almost constant at an intermediate level (e.g., Gosling et al., 1981). The intermediate averages of A(He) during the declining phase in Figure 7 are consistent with this observation.

The variation of average interplanetary magnetic field magnitude over the past solar cycle is shown in Figure 8, from King (1981). There are clear minima at the two solar minima, consistent with the near proximity of the heliospheric current sheet at that time. Although Borrini et al. (1981) state that no pattern was apparent in the superposed epoch analysis of field strength in the streamer belt surrounding the current sheet, in analogy with the current sheet embedded in Earth's plasma sheet, one might expect generally depressed field strength there.

During solar maximum, the frequent occurrence of coronal transients should give rise to high averages of field magnitude, as it does for helium, since the field magnitude is elevated in magnetic clouds. This appears to be the case for the present solar cycle, indicated by the 1978 and 1979 averages in Figure 8 and as presented by Slavin and Smith (in these Proceedings). However, the cycle 20 maximum has only intermediate field magnitude averages. This lack of a maximum may be simply a problem of comparing relative values. As has been argued on the basis of geomagnetic records (e.g., Ol', 1971; Feynman, 1982), each individual sunspot cycle should begin with the declining phase, and relative values of a parameter should be compared from there. If the beginning of the present cycle
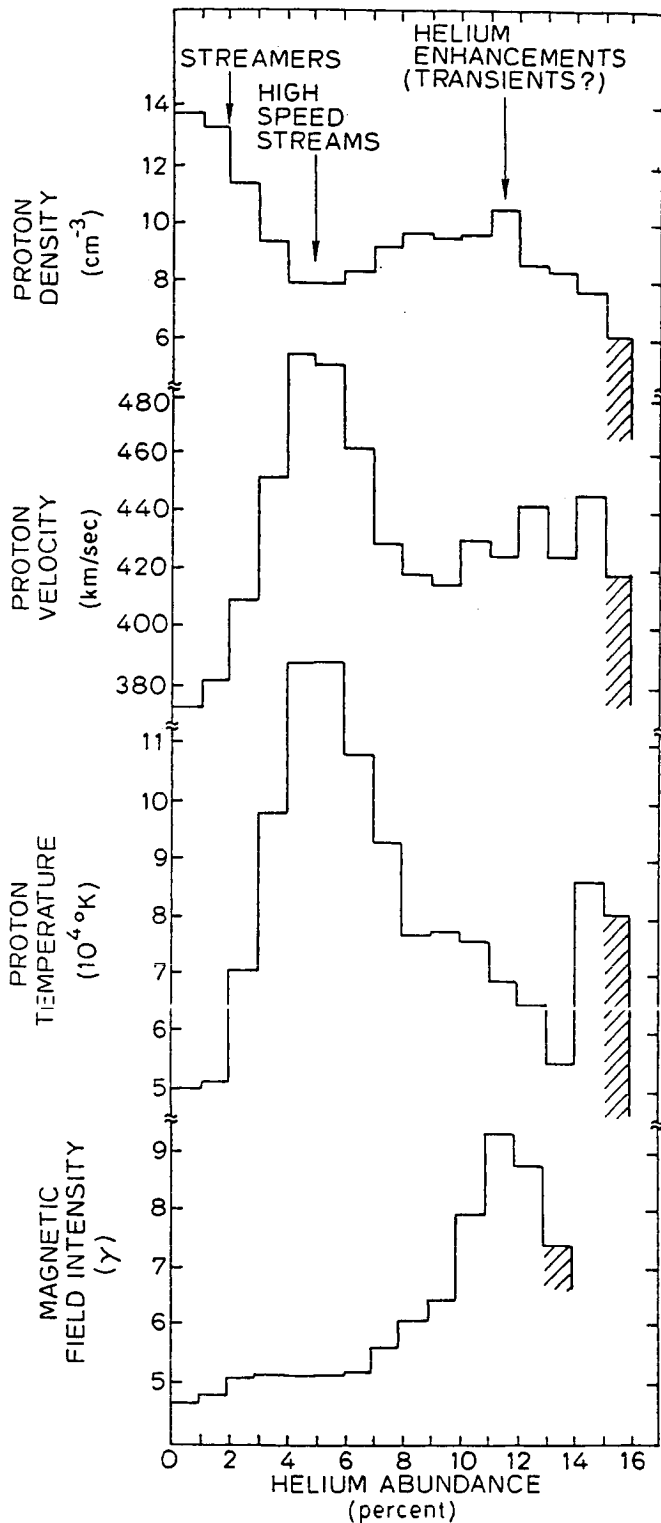
310

Figure 9. Solar wind parameters plotted against relative helium abundance, after Borrini et al. (1983). The shaded end bars include all case of helium abundance higher than 16%.

is set back to include the declining phase of cycle 20, then the magnetic field values there are intermediate between those of the following minimum and maximum phases, in phase with the sunspot cycle.

SUMMARY

Figure 9 is a summary plot from Borrini et al. (1983), upon which this topical review is a generalization. Helium abundance is used as a key to organizing the signatures of the three coronal structures which influence different phases of the solar cycle. Low values of helium correspond to the characteristics of streamers at solar minimum, intermediate values to characteristics of high speed streams during the declining phase, and high values to characteristics of coronal transients at solar maximum.

A summary of solar cycle variations in simple tabular form is given in Table 1. From descending to minimum phase of the sunspot cycle, the signatures of the coronal features characteristic of each phase produce the indicated relative values of solar wind parameters. Briefly stated, the velocity and proton temperature vary together, with maxima in the declining phase, and are anticorrelated with the density and electron temperature, while the helium abundance and magnetic field strength follow the pattern of the sunspot cycle. Of course these patterns are approximate and vary in detail, with some time lag between the solar wind cycle and the sunspot cycle. Nevertheless, it is somewhat remarkable to find that the solar wind parameters follow such a simple, first-order pattern.

Table 1. Summary of Solar Wind Parameters

SUNSPOT CYCLE PHASE	descending	minimum	maximum
CORONAL FEATURES	stable holes	streamer belt	transients
SOLAR WIND			
V, T_p	high	low	medium
n, T_e	low	high	medium
$A(He)$, $|B|$	medium	low	high

REFERENCES

Bame, S. J., J. R. Asbridge, W. C. Feldman, and J. T. Gosling, Solar cycle evolution of high-speed solar wind streams, Astrophys. J., 207, 977-980, 1976.

Borrini, G., J. T. Gosling, S. J. Bame, W. C. Feldman, and J. M. Wilcox, Solar wind helium and hydrogen structure near the heliospheric current sheet: A signal of coronal streamers at 1 AU, J. Geophys. Res., 86, 4565-4573, 1981.

Borrini, G., J. T. Gosling, S. J. Bame, and W. C. Feldman, An analysis of shock wave disturbances observed at 1 AU from 1971 through 1978, J. Geophys. Res., 87, 4365-4373, 1982a.

Borrini, G., J. T. Gosling, S. J. Bame, and W. C. Feldman, Helium abundance enhancements in the solar wind, J. Geophys. Res., 87, 7370-7378, 1982b.

Borrini, G., J. T. Gosling, S. J. Bame, and W. C. Feldman, Helium abundance variations in the solar wind, Solar Phys., in press, 1983.

Feldman, W. C., J. R. Asbridge, S. J. Bame, and J. T. Gosling, Long-term solar wind electron variations between 1971 and 1978, J. Geophys. Res., 84, 7371-7377, 1979.

Feldman, W. C., J. R. Asbridge, S. J. Bame, E. E. Fenimore, and J. T. Gosling, The solar origins of solar wind interstream flows: Near-equatorial coronal streamers, J. Geophys. Res., 86, 5408-5416, 1981.

Feynman, J., Geomagnetic and solar wind cycles, 1900-1975, J. Geophys. Res., 87, 6153-6162, 1982.

Gosling, J. T., E. Hildner, R. M. MacQueen, R. H. Munro, A. I. Poland, and C. L. Ross, Mass ejections from the sun: A view from Skylab, J. Geophys. Res., 79, 4581-4587, 1974.

Gosling, J. T., J. R. Asbridge, S. J. Bame, and W. C. Feldman, Solar wind speed variations: 1962-1974, J. Geophys. Res., 81, 5061-5070, 1976.

Gosling, J. T., E. Hildner, J. R. Asbridge, S. J. Bame, and W. C. Feldman, Noncompressive density enhancements, J. Geophys. Res., 82, 5005-5010, 1977.

Gosling, J. T., G. Borrini, J. R. Asbridge, S. J. Bame, W. C. Feldman, and R. T. Hansen, Coronal streamers in the solar wind at 1 AU, J. Geophys. Res., 86, 5438-5448, 1981.

Hildner, E., J. T. Gosling, R. M. MacQueen, R. H. Munro, A. I. Poland, and C. L. Ross, Frequency of coronal transients and solar activity, Solar Phys., 48, 127-135, 1976.

Hundhausen, A. J., Coronal Expansion and Solar Wind, p. 192, Springer-Verlag, New York, 1972.

Hundhausen, A. J., An interplanetary view of coronal holes, in Coronal Holes and

High Speed Wind Streams, edited by J. B. Zirker, Colorado Associated University Press, Boulder, pp. 225-329, 1977.

Hundhausen, A. J., Solar activity and the solar wind, Rev. Geophys. Space Phys., 17, 2034-2048, 1979.

Hundhausen, A. J., R. T. Hansen, and S. F. Hansen, Coronal evolution during the sunspot cycle: Coronal holes observed with the Mauna Loa K-coronameters, J. Geophys. Res., 86, 2079-2094, 1981.

King, J. H., On the enhancement of the IMF magnitude during 1978-1979, J. Geophys. Res., 86, 4828-4830, 1981.

Klein, L. W., and L. F. Burlaga, Interplanetary magnetic clouds at 1 AU, J. Geophys. Res., 87, 613-624, 1982.

Krieger, A. S., A. F. Timothy, and E. C. Roelof, A coronal hole and its identification as the source of a high velocity solar wind stream, Solar Phys., 29, 505-525, 1973.

Newkirk, G., Jr., A. J. Hundhausen, and V. Pizzo, Solar cycle modulation of galactic cosmic rays: Speculation on the role of coronal transients, J. Geophys. Res., 86, 5387-5396, 1981.

Ogilvie, K. W., and J. Hirshberg, The solar cycle variation of the solar wind helium abundance, J. Geophys. Res., 79, 4595-4602, 1974.

Ol', A. I., Physics of the 11-year variation of magnetic disturbances, Geomag. Aeron., 11, 549-551, 1971.

Russell, C. T., R. L. McPherron, and R. K. Burton, On the cause of geomagnetic storms, J. Geophys. Res., 79, 1105-1109, 1974.

Schulz, M., Interplanetary sector structure and the heliomagnetic equator, Astrophys. Space Sci., 24, 371-383, 1973.

Smith, E. J., B. T. Tsurutani, and R. L. Rosenberg, Observations of the interplanetary sector structure up to heliographic latitudes of 16°: Pioneer 11, J. Geophys. Res., 83, 717-724, 1978.

Smith, E. J., Observations of interplanetary shocks: Recent progress, Space Sci. Rev., in press, 1983.

Svalgaard, L., J. M. Wilcox, P. H. Scherrer, and R. Howard, The sun's magnetic sector structure, Solar Phys., 45, 83-91, 1975.

Zirker, J. B., editor, Coronal Holes and High Speed Wind Streams, Colorado Associated University Press, Boulder, 1977.